

Oblique propagation of electrostatic waves in a magnetized EPI plasma

M. Sarker^{1,a}, B. Hosen², M. G. Shah³, M. R. Hossen⁴, and A. A. Mamun⁵

^{1,2,5}*Department of Physics, Jahangirnagar University,
Savar, Dhaka-1342, Bangladesh*

³*Department of Physics,*

Hajee Mohammad Danesh Science and Technology University, Bangladesh

⁴*Department of General Educational Development,*

Daffodil International University,

Dhanmondi, Dhaka-1207, Bangladesh

Email: ^asarker.plasma@gmail.com

A theoretical investigation is carried out to understand the basic features of nonlinear propagation of heavy ion-acoustic (HIA) waves subjected to an external magnetic field in an electron-positron-ion (EPI) plasma which consists of cold magnetized positively charged heavy ion fluids, and superthermal distributed electrons and positrons. In the nonlinear regime, the Korteweg-de Vries (K-dV) and modified K-dV(MK-dV) equations describing the propagation of HIA waves are derived. The latter admits a solitary wave solution with both positive and negative potentials (for K-dV equation) and only positive potential (for mK-dV equation) in the weak amplitude limit. It is observed that the effects of external magnetic field (obliqueness), superthermal electrons and positrons, different plasma species concentration, heavy ion dynamics and temperature ratio significantly modify the basic features of solitary waves (SWs). The application of the results in a magnetized EPI plasma, which occurs in many astrophysical objects (e.g., pulsars, cluster explosions, and active galactic nuclei) is briefly discussed.

Keywords: HIA SWs; Superthermality Effect; Obliquity on Magnetized Plasmas

I. INTRODUCTION

The perusal of electron-positron-ion (EPI) plasmas is very significant for the understanding of astrophysical as well as celestial environment. The propagation of linear and nonlinear waves in such EPI plasmas has drawn a considerable attention to many authors [1–12]. In most astrophysical and terrestrial environments (viz. white dwarfs, Van Allen belts, etc.), positrons coexist with an admixture of electrons and ions to form EPI plasma, which was found by many researchers [13–18]. It was noticed that plasma system with positron components behave differently than regular two component electron-ion (EI) plasmas. The existence of EPI plasmas has been affirmed in supernovas, pulsar environments, cluster explosions, active galactic nuclei ([12, 19, 20]), at the center of Milky Way galaxy [21], and in the early universe [22].

For modeling purposes, the particle distribution, mostly envisaged to be Maxwellian, when it is very near to equilibrium in a plasma system. On the basis of isothermal assumption, many authors studied the ion acoustic waves in EPI plasmas and most of the studies were concerned with Maxwellian distribution [23–27]. The electrons and positrons which are present in space and astrophysical plasma environments are not in thermal equilibrium but highly energetic [28, 29] due to the effect of external forces or to wave particle interaction in numerous space plasma observations [30, 31] and laboratory experiments [32, 33]. These experiments substantiate the existence of accelerated, highly energetic (superthermal) particles in EPI plasmas. Since the ion temperature is different from the electron and positron

temperature, so an EPI plasma system which is not in thermodynamic equilibrium does not follow a Maxwell-Boltzmann distribution. Plasmas with an excess of superthermal electrons or positrons elicit a deviation from Maxwellian equilibrium [31, 34, 35]. So Maxwell-Boltzmann distribution is not appropriate for explicating the interaction of superthermal particles. However, the plasma system, containing higher energetic (superthermal) particle with energies greater than the energies of the particles, exists in thermal equilibrium that can be fitted more appropriately via the κ (kappa) type of Lorentzian distribution function (DF) [36–38] than via the thermal Maxwellian DF where the real parameter κ measures the deviation from a Maxwellian distribution (the smaller the value, the larger the deviation from a Maxwellian, in fact attained for infinite κ). Shah *et al.* [39] considered an EPI plasma containing inertial ions, superthermal (κ distributed) electrons, and positrons and studied the effect of positron beam on the ion acoustic shock waves. Hence we focus on a plasma system with superthermal particles modelled by a κ -distribution [38].

The three-dimensional (3D) kappa (κ) velocity distribution of particles of mass m is of the form

$$F_k(v) = \frac{\Gamma(k+1)}{(\pi k \omega)^{(3/2)} \Gamma(k-1/2)} \left(1 + \frac{v^2}{k \omega^2}\right)^{-(k+1)}, \quad (1)$$

where, F_k symbolizes the kappa distribution function, Γ is the gamma function, ω shows the most probable speed of the energetic particles, given by $\omega = [(2k-3/k)^{1/2} (k_B T/m)^{1/2}]$, with T being the characteristic kinetic temperature and ω is related to the thermal speed $V_t = (k_B T/m)^{1/2}$ and, the parameter k represents the

spectral index [40] which defines the strength of the superthermality. The range of this parameter is $3/2 < k < \infty$ [41]. In the limit $k \rightarrow \infty$ [42, 43] the kappa distribution function reduces to the well-known Maxwell-Boltzmann distribution.

In last few decades, a number of investigations have been made on the nonlinear propagation of different waves including ion-acoustic (IA), dust ion-acoustic (DIA), heavy ion-acoustic (HIA) waves [44–50]. Cairns *et al.* [48] studied a magnetized plasma system and observed the effects of external magnetic field, obliqueness and ion temperature on the amplitude and width of the IA solitons. Shahmansouri and Alinejad [46] observed the linear and nonlinear excitation of arbitrary amplitude IA solitary waves (SWs) in a magnetized plasma consisting of two-temperature electrons and cold ions. Jilani *et al.* [51] studied the IA solitons in EPI plasma with non-thermal electrons. Baluku and Hellberg [52] examined the arbitrary amplitude IA SWs and double layers (DLs) by using the Sagdeev potential approach in an EPI plasma containing Cairns-distributed (nonthermal) electrons, Boltzmann positrons and cold ion. Pakzad [53] investigated a dissipative plasma system with superthermal electrons and positrons and, observed the effects of ion kinematic viscosity and the superthermal parameter on the IA waves. Ghosh *et al.* [54] studied the nonplanar IA shock waves in a homogeneous unmagnetized EPI plasma containing superthermal electrons, positrons, and singly charged hot positive ions. The existence of positively and negatively charged heavy ions, dust of opposite polarities has been shown to exist in astrophysical environments [47, 55, 56]. Baluku [57] studied the behaviour and existence of DIA waves in a plasma having both polarities of dust. The differences between HIA waves and DIA waves in plasmas are as follows: (a) the frequency of HIA waves is much smaller than that of DIA waves; (b) in DIA waves, static dust grains participate only in maintaining the equilibrium charge neutrality condition, whereas in HIA waves, mobile heavy ions provide the necessary inertia; and (c) in DIA waves, the inertia is provided by the light ions mass, whereas in HIA waves, inertia comes from the heavy ion mass. Hossen *et al.* [58] examined the characteristics of HIA solitary structures associated with the nonlinear electrostatic perturbations in an unmagnetized, collisionless dense plasma.

To the best of our knowledge, no theoretical investigations have been made on the propagation of HIA waves by deriving the magnetized Korteweg-de Vries (K-dV) and magnetized modified K-dV (mK-dV) equations to understand the nonlinear excitations in plasmas containing superthermal electrons and positrons, and heavy ions. In addition, the solitary wave solution of magnetized K-dV and mK-dV equations as well as other parameters like polarity, nonlinearity and dispersion coefficients with amplitude and width of the solitary structures have been studied for different relevant parameters. The manuscript is organized as follows. The basic equations are provided in section II. Two different types of nonlin-

ear equations, namely K-dV and mK-dV are derived and analyzed analytically and numerically in section III. A brief discussion is finally presented in section IV.

II. BASIC EQUATIONS

We consider a three component magnetized plasma system containing positively charged heavy ions and kappa distributed electrons and positrons with two distinct temperatures T_e and T_p . Therefore, at equilibrium condition, $Z_h n_{h0} = n_{e0} + n_{p0}$, where Z_h (n_{h0}) is charge state (equilibrium number density) of the heavy ion species, and n_{e0} (n_{p0}) is the equilibrium electron (positron) number density at temperature T_e (T_p). The dynamics of the heavy ion-acoustic waves, whose phase speed is much smaller (larger) than electron (heavy ion) thermal speed, is described by the normalized equations in the form

$$\frac{\partial n_h}{\partial t} + \nabla \cdot (n_h \mathbf{u}_h) = 0, \quad (2)$$

$$\frac{\partial \mathbf{u}_h}{\partial t} + (\mathbf{u}_h \cdot \nabla) \mathbf{u}_h = -\nabla \phi + \alpha (\mathbf{u}_h \times \hat{z}), \quad (3)$$

$$\nabla^2 \phi = \mu_0 n_e + \mu_1 n_p - n_h, \quad (4)$$

where n_h is the heavy ion number density normalized by n_{h0} ; \mathbf{u}_h is the heavy ion fluid speed normalized by $C_h = (Z_h k_B T_e / m_h)^{1/2}$ (with k_B being the Boltzmann constant, and m_h being the heavy ion mass); ϕ is the electrostatic wave potential normalized by $k_B T_e / e$ (with e being the magnitude of the charge of an electron); $\alpha = \omega_{hc} / \omega_{ph}$ (with $\omega_{ch} = Z_h e B_0 / m_h c$ being the heavy ion-cyclotron frequency, B_0 being the magnitude of the external static magnetic field, c is the speed of light in vacuum, and $\omega_{ph} = (4\pi n_{h0} Z_h^2 e^2 / m_h)^{1/2}$ being the heavy ion plasma frequency); $\mu_0 = \mu / (1 + \mu)$, $\mu_1 = 1 / (1 + \mu)$, and $\mu = n_{e0} / n_{p0}$; n_e (n_p) is the number density of electron (positron); time variable is normalized by ω_{ph}^{-1} , and the space variable is normalized by $\lambda_{Dm} = C_h / \omega_{ph}$. We note that the external magnetic field \mathbf{B}_0 is acting along the z -direction (i.e. $\mathbf{B}_0 = \hat{z} B_0$, where \hat{z} is the unit vector along the z -direction). The normalized electron and positron number densities n_e and n_p are, respectively given by

$$n_e = \left(1 - \frac{\phi}{\kappa_1 - \frac{3}{2}} \right)^{-\kappa_1 + \frac{1}{2}}, \quad (5)$$

$$n_p = \left(1 - \frac{\sigma \phi}{\kappa_2 - \frac{3}{2}} \right)^{-\kappa_2 + \frac{1}{2}}, \quad (6)$$

where $\sigma = T_e / T_p$, κ_1 (κ_2) is the spectral index of superthermal electron (positron).

III. NONLINEAR EQUATIONS

To study nonlinear propagation, we now consider different orders of nonlinearity by deriving and analyzing

K-dV and MK-dV equations to identify the basic features of HIA SWs formed a magnetized space plasma system containing dynamical heavy ions, and kappa distributed electrons and positrons of two distinct temperatures.

A. K-dV Equation

To derive the K-dV equation, we use the reductive perturbation method which leads to the stretched coordinates [59]:

$$\xi = \epsilon^{1/2}(l_x x + l_y y + l_z z - V_p t), \quad (7)$$

$$\tau = \epsilon^{3/2} t, \quad (8)$$

where V_p is the phase speed of the HIA SWs, ϵ is a smallness parameter measuring the weakness of the dispersion ($0 < \epsilon < 1$), and l_x , l_y , and l_z are the directional cosines of the wave vector \mathbf{k} (so that $l_x^2 + l_y^2 + l_z^2 = 1$), as well as leads to the expansion of the perturbed quantities n_h , u_h , and ϕ in power series of ϵ :

$$n_h = 1 + \epsilon n_h^{(1)} + \epsilon^2 n_h^{(2)} + \dots, \quad (9)$$

$$u_{hx,y} = 0 + \epsilon^{3/2} u_{hx,y}^{(1)} + \epsilon^2 u_{hx,y}^{(2)} + \dots, \quad (10)$$

$$u_{hz} = 0 + \epsilon u_{hz}^{(1)} + \epsilon^2 u_{hz}^{(2)} + \dots, \quad (11)$$

$$\phi = 0 + \epsilon \phi^{(1)} + \epsilon^2 \phi^{(2)} + \dots. \quad (12)$$

Now, substituting Eqs. (7)–(12) into Eqs. (2)–(4), and then taking the terms containing $\epsilon^{3/2}$ from Eqs. (2) and (3), and ϵ from Eq. (4), we obtain

$$u_{hx}^{(1)} = -\frac{l_y}{\alpha} \frac{\partial \phi^{(1)}}{\partial \xi}, \quad (13)$$

$$u_{hy}^{(1)} = \frac{l_x}{\alpha} \frac{\partial \phi^{(1)}}{\partial \xi}, \quad (14)$$

$$u_{hz}^{(1)} = l_z \frac{\phi^{(1)}}{V_p}, \quad (15)$$

$$n_h^{(1)} = l_z^2 \frac{\phi^{(1)}}{V_p^2}, \quad (16)$$

$$V_p = \frac{l_z}{\sqrt{\mu_0 c_1 - \mu_1 d_1}}, \quad (17)$$

where

$$c_1 = \frac{(2\kappa_1 - 1)}{2\kappa_1 - 3}, \quad (18)$$

$$d_1 = \frac{(2\kappa_2 - 1)\sigma}{2\kappa_2 - 3}. \quad (19)$$

We note that Eq. (17) describes the linear dispersion relation for the propagation of the HIA SWs in the magnetized plasma under consideration and that $l_z = \cos \delta$ (where δ is the angle between the directions of external magnetic field and wave propagation). To the next

higher order of ϵ , we again substitute Eqs. (7)–(12) into Eqs. (2), z-component of Eq. (3), and Eq.(4) and take the terms containing $\epsilon^{5/2}$ from Eq. (2) and z-component of Eq. (3), and ϵ^2 from Eq. (4). We then use Eqs. (13)–(17) to obtain a set of equations in the form

$$\begin{aligned} & \frac{\partial n_h^{(1)}}{\partial \tau} - v_p \frac{\partial n_h^{(2)}}{\partial \xi} + l_x \frac{\partial u_{hx}^{(2)}}{\partial \xi} \\ & + l_y \frac{\partial u_{hy}^{(2)}}{\partial \xi} + l_z \frac{\partial u_{hz}^{(2)}}{\partial \xi} + l_z \frac{\partial (n_h^{(1)} u_{hz}^{(1)})}{\partial \xi} = 0, \end{aligned} \quad (20)$$

$$\frac{\partial u_{hz}^{(1)}}{\partial \tau} - V_p \frac{\partial u_{hz}^{(2)}}{\partial \xi} + l_z u_{hz}^{(1)} \frac{\partial u_{hz}^{(1)}}{\partial \xi} + l_z \frac{\partial \phi_2}{\partial \xi} = 0, \quad (21)$$

$$\begin{aligned} & \frac{\partial^2 \phi_1}{\partial \xi^2} = \mu_0 c_1 \phi^{(2)} + \mu_0 c_2 \phi^{(1)2} \\ & - \mu_1 d_1 \phi^{(2)} - \mu_1 d_2 \phi^{(1)2} - n_h^{(2)}. \end{aligned} \quad (22)$$

where

$$c_2 = \frac{(2\kappa_1 - 1)(2\kappa_1 + 1)}{2(\kappa_1 - 3)^2}, \quad (23)$$

$$d_2 = \frac{(2\kappa_2 - 1)(2\kappa_2 + 1)\sigma^2}{2(\kappa_2 - 3)^2}. \quad (24)$$

On the other-hand, substituting Eqs. (7)–(12) into x - and y - components of Eq. (3), and taking the terms containing ϵ^2 , we get

$$u_{hy}^{(2)} = \frac{l_y V_p}{\alpha^2} \frac{\partial^2 \phi^{(1)}}{\partial \xi^2}, \quad (25)$$

$$u_{hx}^{(2)} = \frac{l_x V_p}{\alpha^2} \frac{\partial^2 \phi^{(1)}}{\partial \xi^2}. \quad (26)$$

Now combining the equation (20)–(26), we have a equation of the form

$$\frac{\partial \phi^{(1)}}{\partial \tau} + A_1 \phi^{(1)} \frac{\partial \phi^{(1)}}{\partial \xi} + B_1 \frac{\partial^3 \phi^{(1)}}{\partial \xi^3} = 0. \quad (27)$$

where

$$A_1 = \frac{3l_z^2}{2V_p} - V_p, \quad (28)$$

$$B_1 = \frac{V_p^3}{2l_z^2} \left[1 + \frac{(1 - l_z^2)}{\alpha^2} \right]. \quad (29)$$

Equation (27) is the K-dV equation describing the non-linear dynamics of the HIA SWs. Now, using the appropriate boundary conditions, viz. $\phi = 0$, $d\phi/d\xi = 0$, and $d^2\phi/d\xi^2 = 0$ at $\xi \rightarrow \pm\infty$, the stationary solitary wave solution of Eq. (27) is given by

$$\phi^{(1)} = \phi_m \left[\text{sech}^2 \left(\frac{\xi}{\Delta} \right) \right], \quad (30)$$

where $\phi_m = 3u_0/A_1$ is the amplitude, and $\Delta = (4B_1/u_0)^{1/2}$ is the width of the HIA SWs. To obtain

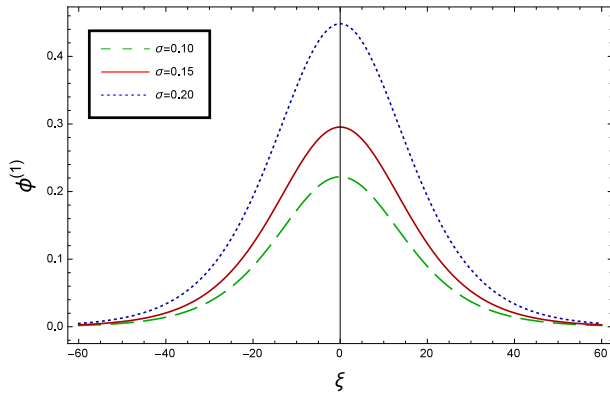


FIG. 1: (Color online) The electrostatic solitary potential profiles (ESPPs) with $\phi^{(1)} > 0$ for $\mu > \mu_c$, $u_0 = 0.01$, $\mu = 2.98$, $\kappa_1 = 20$, $\kappa_2 = 3$, $\delta = 15$, $\alpha = 0.5$, $\sigma = 0.10$ (dashed curve), $\sigma = 0.15$ (solid curve), and $\sigma = 0.20$ (dotted curve).

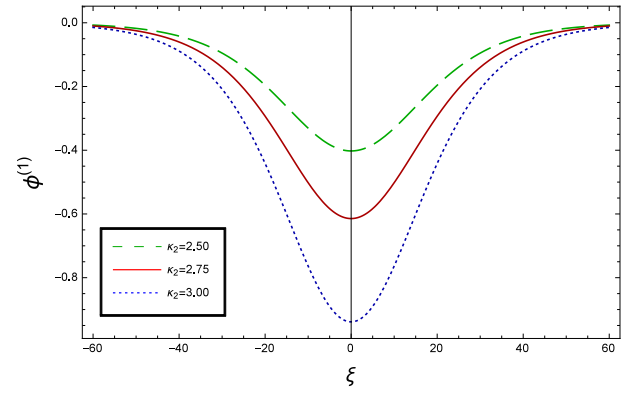


FIG. 4: (Color online) The ESPPs with $\phi^{(1)} < 0$ for $\mu < \mu_c$, $u_0 = 0.01$, $\sigma = 0.25$, $\mu = 2.63$, $\kappa_1 = 20$, $\delta = 15$, $\alpha = 0.5$, $\kappa_2 = 2.50$ (dashed curve), $\kappa_2 = 2.75$ (solid curve), and $\kappa_2 = 3.00$ (dotted curve).

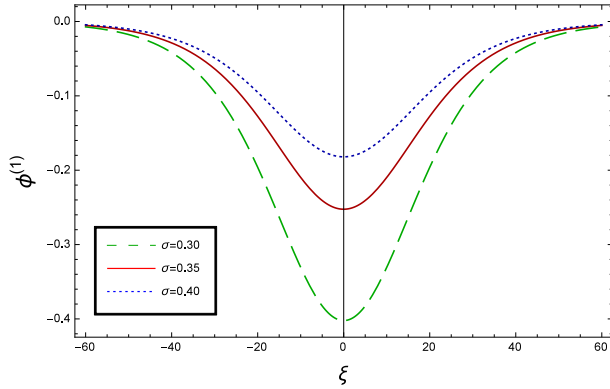


FIG. 2: (Color online) The ESPPs with $\phi^{(1)} < 0$ for $\mu < \mu_c$, $u_0 = 0.01$, $\mu = 2.63$, $\kappa_1 = 20$, $\kappa_2 = 3$, $\delta = 15$, $\alpha = 0.5$, $\sigma = 0.30$ (dashed curve), $\sigma = 0.35$ (solid curve), and $\sigma = 0.40$ (dotted curve).

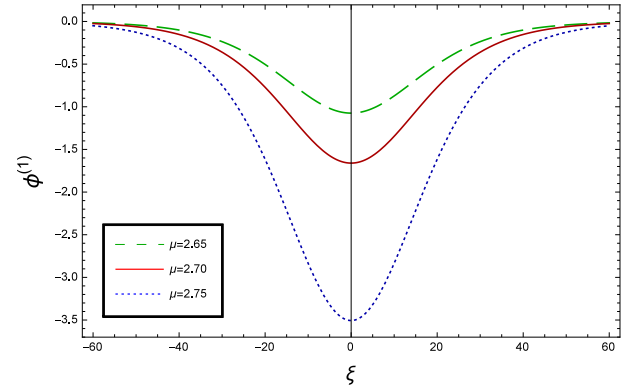


FIG. 5: (Color online) The ESPPs with $\phi^{(1)} < 0$ for $\mu < \mu_c$, $u_0 = 0.01$, $\sigma = 0.25$, $\kappa_1 = 20$, $\kappa_2 = 3$, $\delta = 15$, $\alpha = 0.5$, $\mu = 2.65$ (dashed curve), $\mu = 2.70$ (solid curve), and $\mu = 2.75$ (dotted curve).

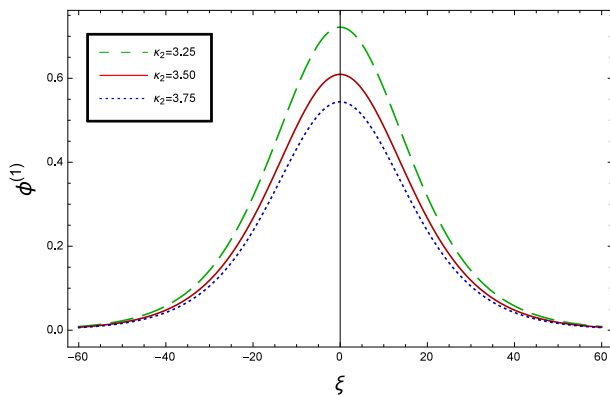


FIG. 3: (Color online) The ESPPs with $\phi^{(1)} > 0$ for $\mu > \mu_c$, $u_0 = 0.01$, $\sigma = 0.25$, $\mu = 2.98$, $\kappa_1 = 20$, $\delta = 15$, $\alpha = 0.5$, $\kappa_2 = 3.25$ (dashed curve), $\kappa_2 = 3.50$ (solid curve), and $\kappa_2 = 3.75$ (dotted curve).

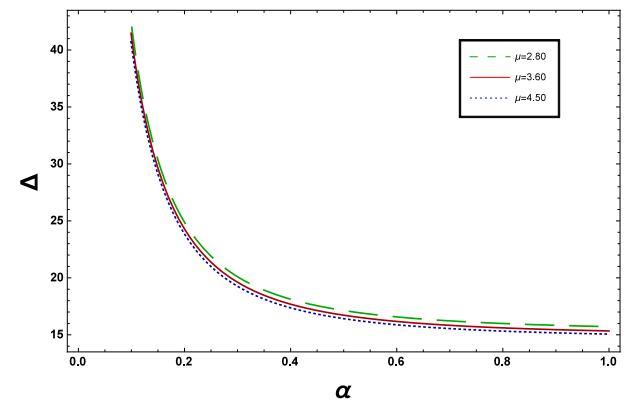


FIG. 6: (Color online) The ESPPs with $\phi^{(1)} > 0$ for $\mu > \mu_c$, $u_0 = 0.01$, $\delta = 15$, $\sigma = 0.25$, $\kappa_1 = 20$, $\kappa_2 = 3$, $\mu = 2.80$ (dashed curve), $\mu = 3.6$ (solid curve), and $\mu = 4.50$ (dotted curve).

the basic features (viz. polarity, amplitude, and width)

of the ESPPs, we have numerically analyzed the solution,

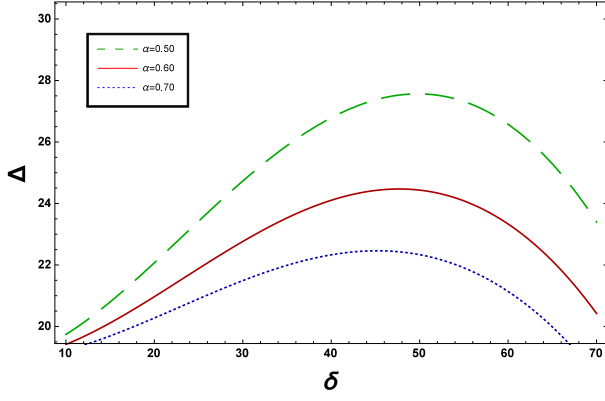


FIG. 7: (Color online) The width of the ESPPs for $\mu > \mu_c$, $u_0 = 0.01$, $\sigma = 0.25$, $\mu = 2.98$, $\kappa_1 = 20$, $\kappa_2 = 3$, $\alpha = 0.5$ (dashed curve), $\alpha = 0.6$ (solid curve), and $\alpha = 0.7$ (dotted curve).

Eq. (30) for different plasma situations. The results are displayed in Figs. 1–7, which clearly indicate that (i) the ESPPs with $\phi^{(1)} > 0$ ($\phi^{(1)} < 0$) exist for $\mu > \mu_c$ ($\mu < \mu_c$) as shown in Figs. 1–5; (ii) the amplitude and width of the ESPPs [with both $\phi^{(1)} > 0$ and $\phi^{(1)} < 0$] increase (decrease) with the increase in σ (κ_2) as shown in Figs. 1–4; (iii) the amplitude of the ESPPs [with $\phi^{(1)} < 0$ for $\mu < \mu_c$] decreases with the increase in μ as shown in Fig. 5; (iv) the width of the ESPPs [with both $\phi^{(1)} > 0$] also decreases slightly with the gradually increase in μ and α as shown in Fig. 6; (v) the width of the ESPPs [with $\phi^{(1)} > 0$] increases (decreases) with the increase in δ for its lower (upper) range, but it decreases with the increase in α as shown in Fig. 7.

B. MK-dV Equation

To derive the MK-dV equation we use the same stretched co-ordinates defined by Eqs. (7) and (8), but the different types of expansion of the dependent variables:

$$n_h = 1 + \epsilon^{1/2} n_h^{(1)} + \epsilon n_h^{(2)} + \epsilon^{3/2} n_h^{(3)} + \dots, \quad (31)$$

$$u_{hx,y} = 0 + \epsilon u_{hx,y}^{(1)} + \epsilon^{3/2} u_{hx,y}^{(2)} + \epsilon^2 u_{hx,y}^{(3)} + \dots, \quad (32)$$

$$u_{hz} = 0 + \epsilon^{1/2} u_{hz}^{(1)} + \epsilon u_{hz}^{(2)} + \epsilon^{3/2} u_{hz}^{(3)} + \dots, \quad (33)$$

$$\phi = 0 + \epsilon^{1/2} \phi^{(1)} + \epsilon \phi^{(2)} + \epsilon^{3/2} \phi^{(3)} \dots, \quad (34)$$

Now, substituting Eqs. (7), (8) and (31)–(34) into Eqs. (2)–(4), and then taking the terms containing ϵ from Eq. (2) and z-component of Eq. (3), and $\epsilon^{1/2}$ from Eq. (4), we find the expressions for $n_h^{(1)}$, $u_{hx}^{(1)}$, $u_{hy}^{(1)}$, $u_{hz}^{(1)}$, V_p , $u_{hx}^{(2)}$, and $u_{hy}^{(2)}$ which have already been given by Eqs. (13)–(17), (25), and (26). To the next higher order of ϵ , again we substitute Eqs. (7), (8) and (31)–(34) into Eqs. (2)–(4), and take the terms containing $\epsilon^{3/2}$ from Eq. (2) and the z-component of Eq. (3), and ϵ from Eq. (4).

Then using the expressions for $n_h^{(1)}$, $u_{hx}^{(1)}$, $u_{hy}^{(1)}$, $u_{hz}^{(1)}$, V_p , $u_{hx}^{(2)}$, and $u_{hy}^{(2)}$ in these higher order equations, we obtain a set of equations:

$$u_{hz}^{(2)} = \frac{l_z^3 \phi^{(1)2}}{2V_p^3} + \frac{l_z \phi^{(2)}}{V_p}, \quad (35)$$

$$n_h^{(2)} = \frac{3l_z^4 \phi^{(1)2}}{2V_p^4} + \frac{l_z^2 \phi^{(2)}}{V_p^2}, \quad (36)$$

$$\rho^{(2)} = -\frac{1}{2} A \phi^{(1)2} = 0, \quad (37)$$

where,

$$A = \left[\frac{3l_z^4}{2V_p^4} - (\mu_0 c_2 - \mu_1 d_2) \right].$$

To further higher order of ϵ , substituting Eqs. (7), (8) and (31)–(34) into Eqs. (2)–(4), and then taking the terms containing ϵ^2 from Eq. (2) and the z-component of Eq. (3), and $\epsilon^{3/2}$ from Eq. (4), we obtain another set of equations:

$$\begin{aligned} & \frac{\partial n_h^{(1)}}{\partial \tau} - V_p \frac{\partial n_h^{(3)}}{\partial \xi} + l_x \frac{\partial u_{hx}^{(2)}}{\partial \xi} + l_x \frac{\partial}{\partial \xi} (n_h^{(1)} u_{hx}^{(1)}) \\ & + l_y \frac{\partial u_{hy}^{(2)}}{\partial \xi} + l_y \frac{\partial}{\partial \xi} (n_h^{(1)} u_{hy}^{(1)}) + l_z \frac{\partial u_{hz}^{(3)}}{\partial \xi} \\ & + l_z \frac{\partial}{\partial \xi} (n_h^{(1)} u_{hz}^{(2)}) + l_z \frac{\partial}{\partial \xi} (n_h^{(2)} u_{hz}^{(1)}) = 0, \end{aligned} \quad (38)$$

$$\frac{\partial u_{hz}^{(1)}}{\partial \tau} - V_p \frac{\partial u_{hz}^{(3)}}{\partial \xi} + l_z \frac{\partial}{\partial \xi} (u_{hz}^{(1)} u_{hz}^{(2)}) + l_z \frac{\partial \phi^{(3)}}{\partial \xi} = 0, \quad (39)$$

$$\begin{aligned} & \frac{\partial^2 \phi^{(1)}}{\partial \xi^2} = (\mu_0 c_1 - \mu_1 d_1) \phi_3 + 2(\mu_0 c_2 \\ & - \mu_1 d_2) \phi^{(1)} \phi^{(2)} - n_h^{(3)}. \end{aligned} \quad (40)$$

Now, combining Eqs. (38)–(40), we finally obtain the mK-dV equation:

$$\frac{\partial \phi^{(1)}}{\partial \tau} + \alpha_1 \alpha_3 \phi^{(1)2} \frac{\partial \phi^{(1)}}{\partial \xi} + \alpha_2 \alpha_3 \frac{\partial^3 \phi^{(1)}}{\partial \xi^3} = 0. \quad (41)$$

where

$$\alpha_1 = \frac{15l_z^6}{2V_p^6}, \quad (42)$$

$$\alpha_2 = 1 + \frac{(1 - L_z^2)}{\alpha^2}, \quad (43)$$

$$\alpha_3 = \frac{V_p^3}{2L_z^2}. \quad (44)$$

To solve this mK-dV equation, We consider a frame $\xi = \eta - u_0 T$ (moving with speed u_0). The stationary solitary wave solution of the MK-dV equation [Eq. (41)] is given by

$$\phi^{(1)} = \phi_m \left[\text{sech} \left(\frac{\xi}{\omega} \right) \right], \quad (45)$$

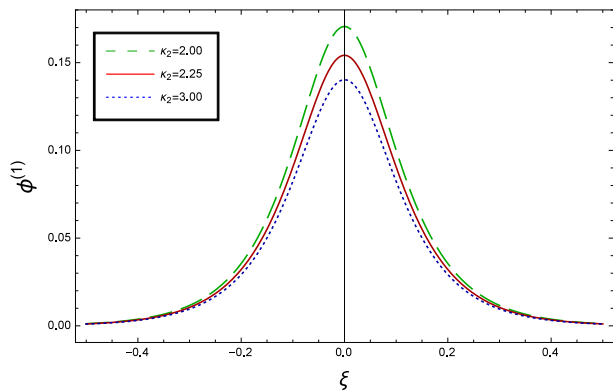


FIG. 8: (Color online) The ESPPs with $\phi^{(1)} > 0$ for $u_0 = 0.01$, $\sigma = 0.25$, $\mu = 2.98$, $\kappa_1 = 20$, $\delta = 15$, $\alpha = 0.5$, $\kappa_2 = 2.00$ (dashed curve), $\kappa_2 = 2.25$ (solid curve), and $\kappa_2 = 3.00$ (dotted curve).

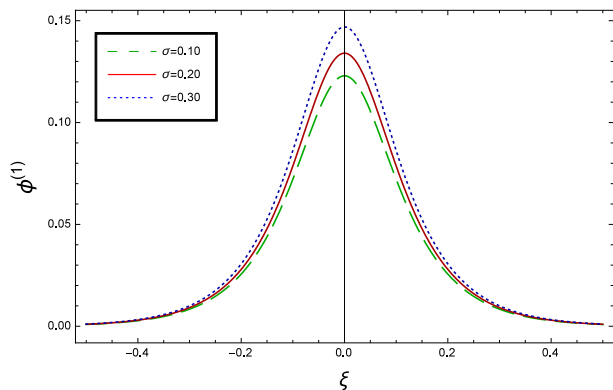


FIG. 9: (Color online) The ESPPs with $\phi^{(1)} > 0$ for $u_0 = 0.01$, $\delta = 15$, $\mu = 2.98$, $\kappa_1 = 20$, $\kappa_2 = 3$, $\alpha = 0.5$, $\sigma = 0.10$ (dashed curve), $\sigma = 0.20$ (solid curve), and $\sigma = 0.30$ (dotted curve).

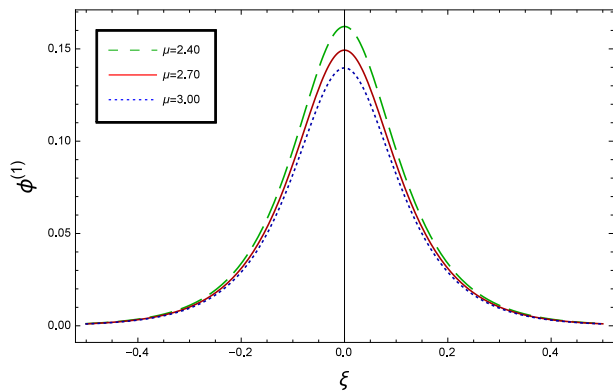


FIG. 10: (Color online) The ESPPs with $\phi^{(1)} > 0$ for $u_0 = 0.01$, $\delta = 15$, $\sigma = 0.25$, $\kappa_1 = 20$, $\kappa_2 = 3$, $\alpha = 0.5$, $\mu = 2.40$ (dashed curve), $\mu = 2.70$ (solid curve), and $\mu = 3.00$ (dotted curve).

where $\phi_m = \sqrt{6u_0/\alpha_1\alpha_3}$ is the amplitude, and $\varpi = \sqrt{u_0/\alpha_3}$ is the width of HIA SWs.

To identify the salient features (viz. polarity, ampli-

tude, and width) of the ESPPs, we have numerically analyzed the solution of the mK-dV equation [Eq. (45)] for different plasma parametric regimes. The results are depicted in Figs. 8–10, which clearly indicates that (i) the mK-dV equation admits solitary wave solution with $\phi^{(1)} > 0$ only; (ii) the amplitude and width of the ESPPs decrease with the increase in κ_2 as shown in Fig. 8; (iii) the amplitude and width of the ESPPs increase with the increase in σ as shown in Fig. 9; (iv) the amplitude and width of the ESPPs decrease with the increase in μ as shown in Fig. 10.

IV. DISCUSSION

We have considered a magnetized plasma system consisting of inertial heavy ions and kappa distributed hot electrons and hot positrons of two distinct temperatures. We have derived the magnetized K-dV and mK-dV-type partial differential equations by using the reductive perturbation method to investigate the basic features (i.e. polarity, amplitude, and width) of such a plasma system. The magnetized K-dV and MK-dV equations are solved to set out the fascinating features of HIA SWs. Then these solutions are analyzed by taking the effect of different plasma parameters. The results, which have been obtained from this theoretical investigation, can be pin-pointed as follows:

1. The K-dV equation admits HIA SW solutions with either $\phi^{(1)} > 0$ (compressive) or $\phi^{(1)} < 0$ (rarefactive). The polarity of the HIA SWs depends on the critical value μ_c (where $\mu_c = 2.98$ for $\kappa_1 = 20$, $\kappa_2 = 3$, $\delta = 15$, $\sigma = 0.25$, and $\alpha = 0.5$). On the other-hand, the MK-dV equation admits only HIA SW solution with $\phi^{(1)} > 0$ (compressive).
2. The K-dV equation is no longer valid at $A_1 \simeq 0$ because the amplitude of the K-dV solitons become infinitely large (for $A_1 = 0$), which has been avoided by deriving MK-dV equation to study more highly nonlinear HIA SWs.
3. The amplitude and width of both positive and negative HIA SWs (obtained from the numerical analysis of the solution of the K-dV equation) increase with the increase in T_e and n_{p0} but decrease with the increase in T_p , n_{eo} , and κ_2 .
4. The width of the K-dV solitons decreases with the increase in α , and increases (decreases) with the increase in δ for its lower (upper) range.
5. The amplitude and the width of the MK-dV HIA SWs decrease with the increase in κ_2 , T_p , and n_{eo} , but increase with the increase in T_e and n_{p0} .

Therefore, we hope that our present investigation would contribute to understand the prime features (i.e. polarity, amplitude, and width) of the electrostatic disturbances of

HIA SWs in a magnetized plasma system. Our findings would be useful to study nonlinear structures in space (viz. peculiar velocities of galaxy clusters, cluster explosions, active galactic nuclei, pulsar magnetosphere, ionosphere [60], Saturns magnetosphere [43], solar wind [61],

etc.) as well as laboratory plasma conditions [12, 62–65] (viz. semiconductor plasmas [66]) containing heavy ions where the effect of two temperature superthermal electrons and positrons play a crucial role.

-
- [1] V. I. Berezhiani, M. Y. El-Ashry, and U. A. Mofiz, *Phys. Rev. E* **50**, 448 (1994).
- [2] S. I. Popel, S. V. Vladimirov, and P. K. Shukla, *Phys. Plasmas* **2**, 716 (1995).
- [3] F. B. Rizzato, *J. Plasma Phys.* **40**, 288 (1998).
- [4] P. K. Shukla, J. T. Mendonca, and R. Bingham, *Phys. Scr.* **113**, 133 (2004).
- [5] A. Mushtaq and H. A. Shah, *Phys. Plasmas* **12**, 072306 (2005).
- [6] W. M. Moslem, I. Kourakis, P. K. Shukla, and R. Schlickeiser, *Phys. Plasmas* **14**, 102901 (2007).
- [7] R. S. Tiwari, A. Kaushik and M. K. Mishra, *Phys. Lett. A* **365**, 335 (2007).
- [8] M. G. Shah, M. R. Hossen, and A. A. Mamun, *Braz. J. Phys.* **45**, 219 (2015).
- [9] M. G. Shah, A. A. Mamun, and M. R. Hossen, *J. Korean Phys. Soc.* **66**, 1239 (2015).
- [10] M. G. Shah, M. R. Hossen, and A. A. Mamun, *J. Plasma Phys.* **81**, 905810517 (2015).
- [11] M. G. Shah, M. R. Hossen, S. Sultana, and A. A. Mamun, *Chin. Phys. Lett.* **32**, 085203 (2015).
- [12] M. Tribeche, K. Aoutou, S. Younsi, and R. Amour, *Phys. Plasmas* **16**, 072103 (2009).
- [13] A. M. Galper, S. V. Koldashov, V. V. Mikhailov, and S. A. Voronov, *Radiation Measurements* **26**, 375 (1996).
- [14] S. A. Voronov, A. M. Galper, V. G. Kirilov-Ugryumov, S. V. Koldashov, and A. V. Popov, *JETP Lett.* **43**, 307 (1986).
- [15] S. L. Shapiro and S. A. Teukolsky, *Black Holes, White Dwarfs and Neutron Stars: The Physics of Compact Objects* (John Wiley, New York, 1983).
- [16] M. R. Hossen and A. A. Mamun, *Braz. J. Phys.* **67**, 458 (2014).
- [17] M. R. Hossen, S. A. Ema, and A. A. Mamun, *Commu. Theo. Phys.* **62**, 888 (2014).
- [18] M. A. Hossen, M. G. Shah, M. R. Hossen, and A. A. Mamun, *Commu. Theo. Phys.* **67**, 458 (2017).
- [19] M. C. Begelman, R. D. Blanford, and M.J. Rees, *Rev. Mod. Phys.* **56**, 255 (1984).
- [20] H. R. Miller, P. J. Witta, *Active Galactic Nuclei* (Springer, Berlin, 1987).
- [21] M. L. Burns, *Positron-electron pairs in astrophysics* (American Institute of Physics, Melville, 1983).
- [22] G. W. Gibbons, S. W. Hawking, and S. Siklos, *The very early universe* (Cambridge University Press, Cambridge, 1983).
- [23] Q. Haque and H. Saleem, *Phys. Plasmas* **10**, 3793 (2003).
- [24] R. Sabry, W. M. Moslem, and P. K. Shukla, *Eur. Phys. J. D* **51**, 233 (2009).
- [25] E. I. El-Awady, S. A. El-Tantawy, W. M. Moslem, and P. K. Shukla, *Phys. Lett. A* **374**, 3216 (2010).
- [26] M. Akbari-Moghanjoughi, *Phys. Plasmas* **17**, 082315 (2010).
- [27] A. Shah, R. Saeed and M. Noaman-Ul-Haq, *Phys. Plasmas* **17**, 072307 (2010).
- [28] A. A. Gusev, U. B. Jayanthi, G. I. Pugacheva, V. M. Pankov, and N. Schuch, *Earth Planets Space* **54**, 707 (2003).
- [29] J. R. Dwyer, B. W. Grefenstette, and D. M. Smith, *Geophys. Res. Lett.* **81**, L02815 (2008).
- [30] C. Vocks and G. Mann *Astrophys. J.* **593**, 1134 (2003).
- [31] G. Gloeckler and L. A. Fisk, *Astrophys. J.* **648**, L63 (2006).
- [32] Y. Yagi, V. Antoni, M. Bagatin, D. Desideri, E. Martines, G. Seriani, and F. Vallone, *Plasma Phys. Cont. Fusion* **39**, 1915 (1997).
- [33] S. Preische, P. C. Efthimion, and S. M. Kaye, *Phys. Plasmas* **3**, 4065 (1996).
- [34] M. Maksimovic, V. Pierrard, and J. F. Lemaire, *Astron. Astrophys.* **324**, 725 (1997).
- [35] C. C. Chaston, Y. D. Hu, and B. J. Fraser, *Geophys. Res. Lett.* **24**, 2913 (1997).
- [36] V. M. Vasyliunas, *J. Geophys. Res.* **73**, 2839 (1968).
- [37] D. Summers and R. M. Thorne, *Phys. Fluids B* **3**, 1835 (1991).
- [38] M. A. Hellberg, R. L. Mace, T. K. Baluku, I. Kourakis, and N. S. Saini, *Phys. Plasmas* **16**, 094701 (2009).
- [39] A. Shah, S. Mahmood, and Q. Haque, *Phys. Plasmas* **19**, 032302 (2012).
- [40] T. Cattaert, M. A. Helberg, and R. L. Mace, *Phys. Plasmas* **14**, 082111 (2007).
- [41] M. S. Alam, M. M. Masud, and A. A. Mamun, *Plasma Phys. Rep.* **39**, 1011 (2013).
- [42] B. Basu, *Phys. Plasmas* **15**, 042108 (2008).
- [43] T. K. Baluku and M. A. Hellberg, *Phys. Plasmas* **19**, 012106 (2012).
- [44] B. Hosen, M. G. Shah, M. R. Hossen, and A. A. Mamun, *Euro. Phys. J. Plus* **131**, 81 (2016).
- [45] M. G. Shah, M. R. Hossen, and A. A. Mamun, *Commun. Theo. Phys.* **64**, 208 (2015).
- [46] M. Shahmansouri and H. Alinejad, *Phys. Plasmas* **20**, 082130 (2013).
- [47] P. K. Shukla and A. A. Mamun, *Introduction to Dusty Plasma Physics* (IOP, Bristol, 2002).
- [48] R. A. Cairns, A. A. Mamun, R. Bingham, and P. K. Shukla, *Phys. Scr.* **T63**, 80 (1996).
- [49] P. K. Shukla and V. P. Silin, *Phys. Scr.* **45**, 508 (1992).
- [50] S. Qian, W. Lotko, and M. K. Hudson, *J. Geophys. Res.*, **94**, 1339 (1989).
- [51] K. Jilani, A. M. Mirza, and T. A. Khan, *Astrophys. Space. Sci.* **344**, 135 (2012).
- [52] T. K. Baluku and M. A. Hellberg, *Plasma Phys. Control. Fusion* **53**, 095007 (2011).
- [53] H. R. Pakzad, *Astrophys. Space Sci.* **331**, 169 (2011).
- [54] D. K. Ghosh, P. Chatterjee, P. K. Mandal, and B. Sahu, *Pramana* **81**, 491 (2013).
- [55] T. A. Ellis and J. S. Neff, *Icarus* **91**, 280 (1991).
- [56] V. W. Chow, D. A. Mendis, and M. Rosenberg, *J. Geo-*

- phys. Res. **98**, 19065 (1993).
- [57] T. K. Baluku, M. A. Hellberg, I. Kourakis, and N. S. Saini, Phys. Plasmas **17**, 053702 (2010).
- [58] M. R. Hossen, L. Nahar, S. Sultana, and A. A. Mamun, Astrophys. Space Sci. **353**, 123 (2014).
- [59] A. A. Mamun, Astrophys. Space Sci. **260**, 507 (1998).
- [60] J. Bremer, P. Hoffmann, A. H. Manson, C. E. Meek, R. Ruster, and W. Singer, Ann. Geophys. **14**, 1317 (1996).
- [61] V. Pierrard and J. Lemaire, J. Geophys. Res. **101**, 7923 (1996).
- [62] C. M. Surko, M. Leventhal, and A. Passner, Phys. Rev. Lett. **62**, 901 (1989).
- [63] K. Abdullah, L. Haarsma, and G. Gabrielse, Phys. Scr. T **59**, 337 (1995).
- [64] C. Kurz, S. J. Gilbert, R. G. Greaves, and C. M. Surko, Nucl. Instrum. Methods Phys. Res. B **143**, 188 (1998).
- [65] R. G. Greaves, S. J. Gilbert, and C. M. Surko, Appl. Surf. Sci. **194**, 56 (2002).
- [66] P. K. Shukla, N. N. Rao, M. Y. Yu, and N. L. Tsintsadze, Phys. Rep. **138**, 1 (1986).